The response of texture features to illuminant rotation

M.J. Chantler and G. McGunnigle

Department of Computing and Electrical Engineering, Heriot-Watt University, Edinburgh, Scotland

M.J.Chantler@hw.ac.uk, http://www.cee.hw.ac.uk/~mjc

Abstract

Rotation of the illuminant source about a subject textured surface can cause catastrophic failure of texture classification schemes. This is due to the variation of texture feature output that can occur when the illuminant direction is varied. This paper uses theory and experiment to show that the outputs of linear texture filters, and their features, are sinusoidal functions of the illuminant's tilt angle.

1. Introduction

Many *image textures* are formed by imaging *three-dimensional* textured surfaces. It is well known that such image textures are a function both of surface topography *and* of the illumination conditions. Several authors have developed schemes that are robust to variations in illuminant intensity [1] and colour [2,3]. However, it has been demonstrated that image texture can also be a function illuminant direction, and that such variations can cause catastrophic failures in classification schemes based on Laws measures, co-occurrence matrices, fractal measures, and Gabor filters [4,5].

In this paper a model of the surface-to-image transfer function [6,7] is used to predict that the outputs of many texture features vary as a sinusoidal function of the illuminant's tilt angle. The class of texture features considered are those that can be modelled as a combination of a linear filter followed by a variance estimator. The image textures considered are those that result from topographical variations in the surface (albedo variations are not taken into account).

2. Theory

This section presents a frequency domain image model. Which we use to develop an expression for texture feature output as a function of tilt angle.

Imaging Geometry

The imaging geometry assumptions are as follows. The test surface is mounted perpendicularly to the camera axis (the *z*-axis). It is illuminated by a point source located at infinity, i.e. the incident vector field is uniform in magnitude and direction throughout the test area. The direction of the illuminant with respect to the texture is defined by two polar co-ordinates: slant and tilt. Slant (σ) is the angle between the camera axis and the illuminant vector; in this work it shall be held constant at 60°. Tilt(τ) refers to the polar angle of the illuminant on a plane normal to the camera axis.

Image Model

Kube and Pentland presented a frequency domain model of the formation of the image from the surface [6]. The most significant assumptions are that: the surface reflectance is Lambertian, there is no self or cast shadowing, the camera model is orthographic and that surface slope angles are small. Using the last assumption to justify a linearisation of the Lambertian equation, Kube and Pentland develop a transfer function linking surface and image spectra. Chantler [7] modified and generalised this to the form shown below (1).

$$I(\omega,\theta) = \omega^2 \cos^2(\theta-\tau)\sin^2(\sigma)S(\omega,\theta) \qquad (1)$$

where

(ω,θ) is the polar form of spatial frequency with θ = 0° being the direction of the *x*-axis.

$I(\omega,\theta)$ is the image power spectrum.

$S(\omega,\theta)$ is the surface power spectrum.

This paper deals with the effects of the $\cos^2(\theta-\tau)$ term; this is directional filter and is independent of radial frequency, ω.

Modelling Texture Feature Output

Many texture features are, or may be approximated by, a combination of a linear filter (often directional) followed by a non-linear operator. Examples of linear texture filters include Gabor, Wavelet, and Laws filters; while the non-linear element often comprises a square (x^2) or absolute ($|x|$), function, followed by a lowpass filter or averaging function.

Feature generation may therefore be modelled as shown below (**Figure 1**).

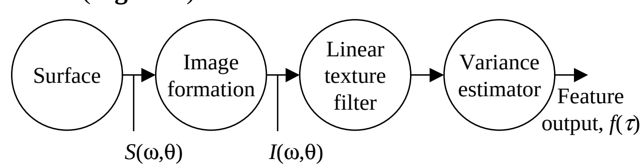

Figure 1 - Texture feature generation

Since the surface-to-image transfer function (1) that we use is linear, the image formation stage and the linear texture filter may be interchanged to provide the model shown below (**Figure 2**).

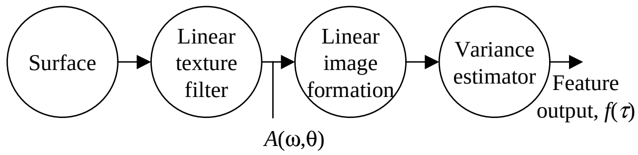

Figure 2 - Texture feature generation: model 2

$A(\omega,\theta)$ is the notional power spectrum of the output of the linear texture filter applied directly to the surface height function. It is therefore unaffected by illuminant tilt.

From (1) the feature output is therefore

$$f(\tau) = \int_0^\infty \omega^2 \sin^2(\sigma).2\int_0^\pi \cos^2(\theta-\tau).A(\omega,\theta).d\theta.d\omega \qquad (2)$$

Now consider the inner integral

$$= 2\int_0^\pi \cos^2(\theta-\tau).A(\omega,\theta).d\theta$$

$$= \int_0^\pi (1+\cos(2\theta-2\tau)).A(\omega,\theta).d\theta$$

$$= \int_0^\pi A(\omega,\theta).d\theta + \int_0^\pi \cos(2\theta-2\tau).A(\omega,\theta).d\theta$$

$$= \int_0^\pi A(\omega,\theta).d\theta + \lim_{n\to\infty}\sum_{i=0}^{i=n-1}\cos(2i\Delta\theta-2\tau).A(\omega,i\Delta\theta)\Delta\theta$$

$$where \quad \Delta\theta = \pi/n$$

With respect to the variable τ, the above summation is simply a series of cosines of varying amplitude and phase but of constant frequency (2τ). A similar argument holds for the outer integral of (2), hence the feature output

$$f(\tau) = a + b\cos(2\tau+\varphi) \qquad (3)$$

where:

$$a = \sin^2(\sigma)\int_0^\infty \omega^2 \int_0^\pi A(\omega,\theta).d\theta.d\omega$$

and b and ϕ are constants.

If the standard deviation is used to calculate the feature value then the output is of the form:

$$f(\tau) = \sqrt{a + b\cos(2\tau+\varphi)} \qquad (4)$$

In either case it can be seen that this model predicts that texture features' outputs vary as the illumination source is rotated about the texture surface.

3. Testing the theoretical predictions

In this section the theoretical prediction (4) is compared with results obtained by applying a set of Gabor features to both computer-generated and real surface textures.

The Texture Features

Gabor filters based on the parameter set defined in [8] were used in our directional features. Jain and Farrokhnia arrange these filters into frequency bands which increase in octaves, each band contains four filters oriented at 0°,45°,90° and 135° respectively. The filters have radial and polar bandwidths of one octave and 45°, respectively. We refer to the directional filters using the form Fω_0dϕ, where ω_0 is the filter's centre frequency in cycles per image, and ϕ is the orientation of the filter in degrees.

In addition to these directional filters we also used a rotation invariant feature. This feature is derived from an isotropic, Gaussian bandpass filter similar to that presented in [9]. Each filter's output was processed with a standard deviation estimator to provide the feature's final output.

Verification by Simulation

Synthetic test images were generated by rendering computer generated height maps using a simple Lambertian shading algorithm. Rendered images of the surfaces, an isotropic fractal and a directional Ogilvy [10] surface are shown below.

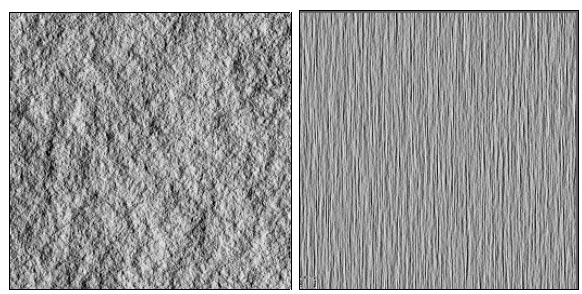

Figure 3 Synthetic fractal (left) and Ogilvy(tight) surfaces

Figure 4 shows the feature output derived from a single F25d0° filter applied to the image of the fractal surface rendered using illuminant tilt angles of between τ = -90° to τ = +90°. A best fit $\sqrt{a+b\cos(2\tau+\varphi)}$ function is plotted on the same graph. The parameters a and b have been estimated using non-linear optimisation.

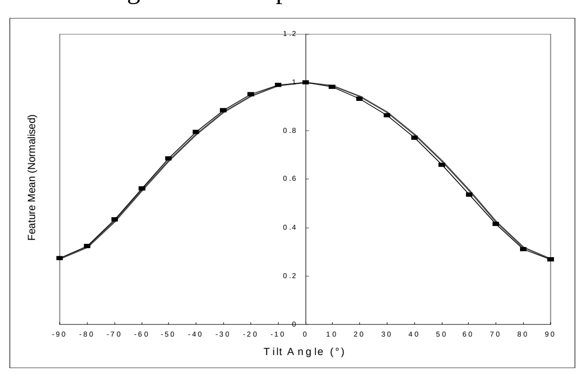

Figure 4 The effect of tilt angle variation on *F25d0°* feature output and best fit cosine (fractal surface)

It can be seen that the output closely approximates the hypothesised cosine function.

In many applications a larger feature set is used. Figure 5 shows the results obtained by applying all the filters of the set within the F25 band (including the isotropic filter). It can be seen that:

(i) the means of the directional features vary sinusoidally with tilt,

(ii) the tilt responses have similar amplitudes,

(iii) the maxima occur when the filter orientation coincides with the tilt angle, i.e. at $\tau=\phi$, and

(iv) the isotropic feature is almost unaffected by tilt variation in the case of an *isotropic* surface.

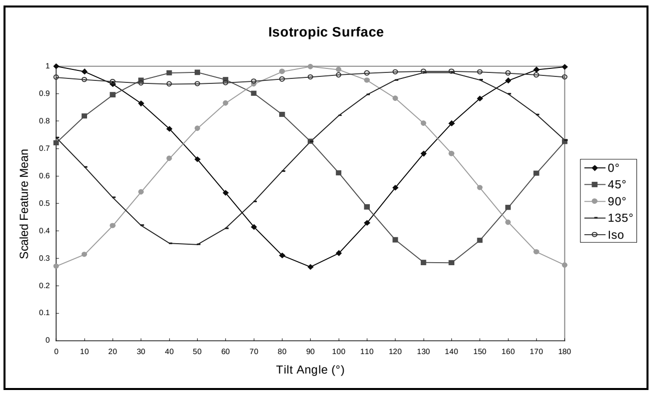

Figure 5 Tilt responses of the F25 filters applied to the images the isotropic fractal surface.

Now consider the effect on feature output of tilt variation on the *directional* Ogilvy surface. In Figure 6 the feature outputs derived from the image of a surface whose directionality is aligned with that of the F25d90 filter are plotted.

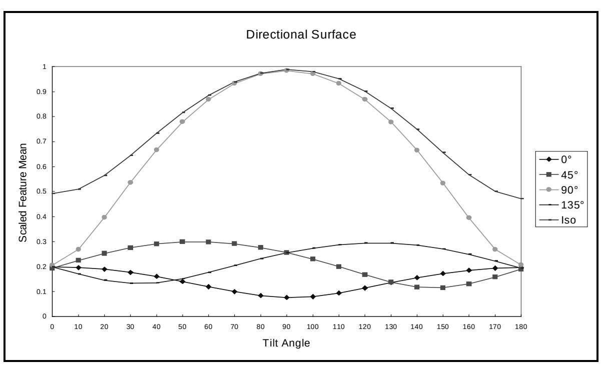

Figure 6 Tilt responses of the F25 features applied to images of the directional surface.

It can be seen that in the case of this directional surface:

(i) the directional features again vary in a sinusoidal manner,

(ii) the output of the isotropic filter varies sinusoidally with tilt—showing that tilt variation is not equivalent to image rotation in the case of a directional surface.

Verification by Experiment

In this section we shall examine results obtained using two real surfaces, *Rock* and *Striate*, shown in Figure 7. *Rock* is isotropic and is similar in appearance to the isotropic fractal. The Striate texture is highly anisotropic, and is closer to the Ogilvy surface.

Images were captured at 10° increments of illuminant tilt. The Striate test sample has been aligned so that the grain of the material is approximately collinear with the $\phi=0°$ filter

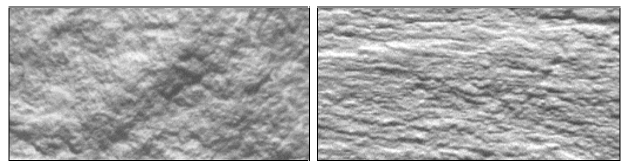

Figure 7 Rock(left) and Striate(right) textures

As with the isotropic synthetic surface, the feature means for the *Rock* texture all vary with tilt in a cosine manner with approximately equal amplitudes.

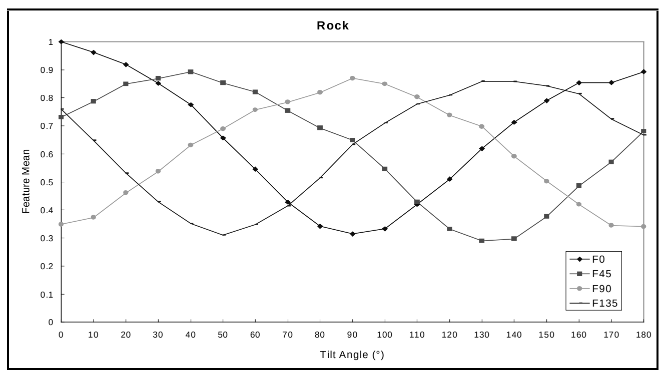

Figure 8 F25 feature responses to 'Rock' surface illuminated at a range of tilt angles.

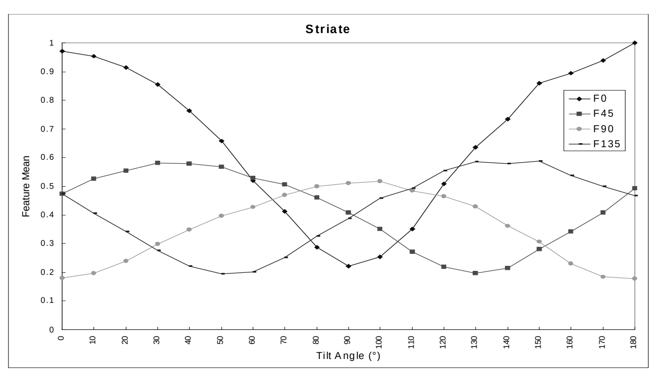

Figure 9 F25 feature responses to 'Striate' surface illuminated at a range of tilt angles.

The results for the 'Striate' texture are similar to those of the Ogilvy surface. As with the synthetic case all features vary in an approximately sinusoidal manner.

Figures 10 & 11 show the tilt responses of the F25d0 and F25d90 features together with best-fit cosine functions.

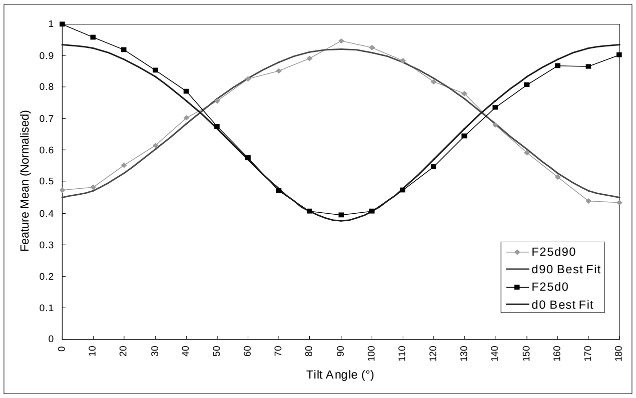

Figure 10 Tilt responses of the F25d0 and F25d90 filters applied to Rock images (with best-fit cosine functions)

These results show that, while the $\sqrt{a + b\cos(2\tau + \varphi)}$ curve is not a perfect model, it does provide a close fit to the experimental data.

It is also clear from the measured results that the features are significantly affected by variations in illuminant tilt. This has serious consequences for classification—a classification rule developed for textures imaged under one illuminant direction may be completely inappropriate for classifying the same surfaces illuminated from a different direction. It has been shown that this may result in catastrophic failure of the classifer [4,5].

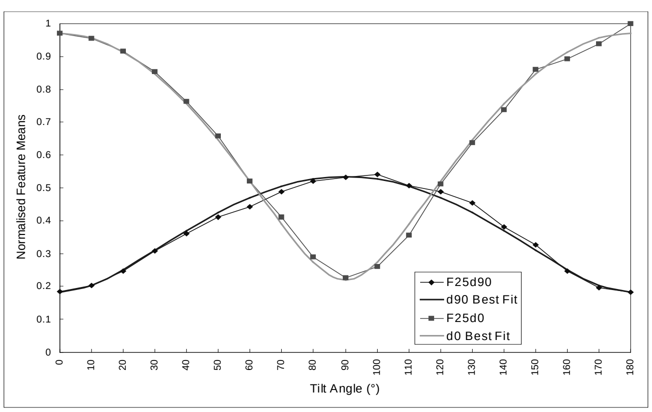

Figure 11 Tilt responses of the F25d0 and F25d90 filters applied to Striate images (shown with best-fit cosine functions)

4. Conclusions

This paper has shown that behaviours of texture features derived from linear filters may be modelled as a sinusoidal function of the illumination's tilt angle (τ).

$$f(\tau) = a + b\cos(2\tau + \varphi)$$

Only in the case where the product of the surface spectrum and the texture filter is isotropic (e.g. isotropic surface and isotropic filter) is the output predicted to be constant (i.e. $b = 0$).

Experiments using Gabor filters applied to synthetic and real surfaces have verified this model.

This has a number of implications for classification. Firstly, classification of textures may be easier when they are illuminated from certain directions, as it may be possible to arrange illumination to improve discrimination. Secondly, changing the direction of illumination after training may result in the derived classification rules being inappropriate to the task in hand. Finally, where rotation invariant classification is required, the rotation of the surface texture *relative to the illuminant direction* introduces changes in the observed textures beyond that of simple image rotation.

References

[1] R.S. Thau "Illuminant Precompensation for Texture Description using Filters", Image Understanding Workshop (DARPA) Pittsburg PA, Sept. 1990 pp.179-184. Publ. Morgan Kaufmann

[2] G. Healey, & L. Wang "Illuminant-Invariant Recognition of Texture in Color Images", Journal of the Optical Society of America, 1995. Vol.12, No.9, pp. 1877-1883.

[3] R. Kondepudy & G. Healey, "Use of invariants for recognition of three-dimensional color textures", Journal of Optical Society of America A, 11 (11), pp.3037-3049, November 1994.

[4] M.J. Chantler, "The effect of illuminant direction on texture classification", PhD Thesis, Heriot-Watt University, 1994.

[5] G. McGunnigle, "The classification of textured surfaces under varying illuminant direction", PhD Thesis, Hierot-Watt University, 1998.

[6] P. Kube & A. Pentland, "On the Imaging of Fractal Surfaces", IEEE Transactions on Pattern Analysis and Machine Intelligence, Vol. 10, No.5, Sept.1988, pp.704-707.

[7] M.J. Chantler, "Why illuminant direction is fundamental to texture analysis", IEE Proceedings: Vision, Image and Signal Processing, Vol. 142, No. 4, August 1995, pp199-206.

[8] A.K. Jain &F. Farrokhnia, "Unsupervised texture segmentation using Gabor filters", Pattern Recognition, Vol.24, No.12 pp. 1167-1186,1991.

[9] R. Porter & N. Canagarajah, "Robust rotation invariant texture classification: Wavelet, Gabor filter and GMRF based schemes", IEE Proc. Vis. Image Signal Process. Vol.144, No.3, June 1997.

[10] J.A. Ogilvy, "Theory of wave scattering from random rough surfaces", 1991, Adam Hilger.